Proton drip line nuclei around $Z=30$ to 40

M. Rajasekaran and Mamta Aggarwal
Department of Nuclear Physics, University of Madras, Guindy Campus, Chennai 600 025, India
(Received 22 June 1998)

Neutron deficient collision products with $Z=30$ to 40 at high excitations are investigated. The proton drip line is significantly altered due to temperature and rotation. The effects of thermal and rotational excitations on proton separation energy are investigated. The level density parameter and the nuclear level density of the isotopes of these fp shell nuclei are also calculated. [S0556-2813(98)07810-8]

PACS number(s): 24.60.−k, 21.10.Ma, 21.10.Dr

I. INTRODUCTION

Recent experiments on proton radioactivity [1,2] around $Z=30$ nuclei [3,4] and identification of nuclei near the proton drip line [5,6] have improved our understanding about these nearly unstable nuclei in which β decay and particle capture compete to establish stability. These neutron-deficient nuclei are usually formed in heavy ion collisions and are in a highly excited state, their decay greatly influenced by thermal and collective excitations. Though several calculations are found in the literature for mapping the drip line nuclei [7–9], like the macroscopic-microscopic [10] method, only a few calculations have included the effects of excitation on the proton and neutron separation energies [11–13] and neutron drip line [14].

In the present article we have investigated the proton drip line nuclei and included both thermal and rotational excitations through the statistical theory [11,12,15–19] while retaining the macroscopic-microscopic method for the ground state nuclei. In view of the very high spins possible in the nucleus formed in collisions, the statistical theory of hot rotating nuclei [20,21] is used here. We present here results for proton drip line nuclei in the region $Z=30$ to 40, which are fp shell nuclei. We find in some cases, $Z=30$, 32, and 38, that thermal excitation pushes the drip line to higher neutron numbers due to nuclear level density fluctuations. The effects of rotation on the separation energy S_p of the last proton is also investigated for these nuclei.

In Sec. II, we present the method of obtaining the ground-state proton separation energy with a macroscopic-microscopic approach for neutron deficient even-even nuclei with $Z=20$ to 70, where we incorporate the Strutinsky shell correction [22–24] to energy into the LDM mass formula of Moller-Nix [25] and obtain the corrected proton separation energy S_p. This is similar to our earlier calculation for the neutron drip line [14]. The locus of the neutron numbers for which $S_p \rightarrow 0$ is the proton drip line. Experimentally, the proton drip line has been mapped by the GANIL group [26] for nuclei below $Z=30$. For $Z=33$, 35, and 37 also, the proton drip line has apparently been reached by the NSCL group [3]. In Sec. III, we introduce the effect of temperature and spin to study the changes in the proton separation energy as well as the proton drip line, with spin and temperature.

II. THE MACROSCOPIC-MICROSCOPIC APPROACH

In the macroscopic method which is based on the liquid drop model (LDM), binding energy varies smoothly with particle number. The macroscopic separation energy can be obtained by taking the difference in LDM binding energies of a system with Z protons and N neutrons in its ground state and the final system of $(Z-1)$ protons and N neutrons, i.e.,

$$S_p^{\mathrm{mac}} = E_{B\ \mathrm{LDM}}(Z,N) - E_{B\ \mathrm{LDM}}(Z-1,N).$$

The macroscopic separation energy has been obtained in our work by using the LDM mass formula of Moller-Nix [25]. The macroscopic separation energy S^{mac} is unable to account for the closed shell discontinuity which arises because of the nonuniform distribution of single particle levels in the nucleus. Nucleon shell effects can be considered as the small deviation from the uniform distribution of nucleons and hence the corresponding correction to macroscopic energy is made which is termed as the shell correction. Contributions to the microscopic term come from the shell correction which is determined by using Strutinsky's shell correction method.

Strutinsky's shell correction to energy can be written as

$$\delta E = \sum_{i=1}^{A} \varepsilon_i - \tilde{E}, \tag{2.1}$$

where the first term is the shell model energy and the second term is the smoothened energy. The smearing width $\gamma \approx 1.2\hbar\omega$ and levels up to $N=11$ shells of the Nilsson model with Seegar parameters [27] are used; this choice ensures that the level scheme is suitable over a wide range of mass number. The single-particle eigenvalues ε_i are different for protons and neutrons (ε_i^Z and ε_i^N). The diagonalization of the Hamiltonian is done using cylindrical basis states [28,29] with Hill-Wheeler [30] deformation parameters (θ,δ). The value of the angular deformation parameter θ ranges from $-180°$ (oblate with symmetry axis parallel to rotation axis) to $-120°$ (prolate with symmetry axis perpendicular to rotation axis). The axial deformation parameter δ ranges from 0 to 0.6.

When the shell correction $\delta E(\theta,\delta)$ for a given deformation is added to macroscopic binding energy E_{LDM} of the spherical nuclei along with the deformation energy E_{def}, we

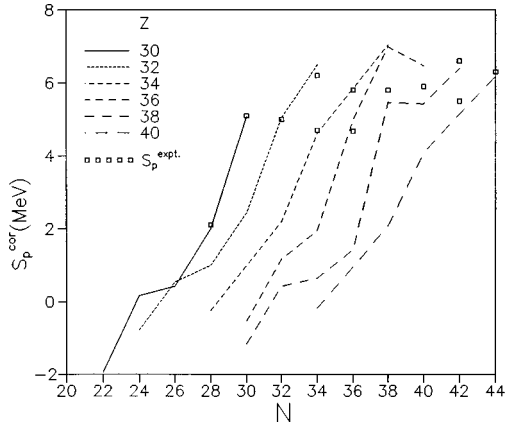

FIG. 1. One proton separation energy $S_p^{\rm cor}$ vs N for Zn, Ge, Se, Kr, Sr, and Zr.

get the total corrected binding energy which is maximized with respect to deformation parameters (θ,δ).

$$E_{B\ \rm tot}(Z,N,\theta,\delta)=E_{B\ \rm LDM}(Z,N) - E_{\rm def}(Z,N,\theta,\delta)-\delta E(Z,N,\theta,\delta). \tag{2.2}$$

The corrected proton separation energy is obtained from

$$S_p^{\rm cor}=E_B(Z,N,\theta,\delta)-E_B(Z-1,N,\theta,\delta), \tag{2.3}$$

or

$$Q=E_B(Z,N,\theta,\delta)-E_B(Z+1,N,\theta,\delta).$$

A positive Q value or a negative S_p indicates the instability of the nucleus against proton radioactivity.

In Fig. 1, S_p vs neutron number is plotted for Zn, Ge, Se, Kr, Sr, and Zr nuclei. The corrected separation energies $S_p^{\rm cor}$ obtained by using Eqs. (2.2) and (2.3) agree very well with the experimental [31] values. We notice that the proton separation energy decreases as neutron number decreases. Owing to the Coulomb term in the mass formula, it is not possible to have nuclei with a very large proton excess and therefore the proton drip line lies rather close to the $N=Z$ line in contrast to the neutron drip line [8,14,32], where the neutron to proton ratio $N/Z=2.3$ approximately.

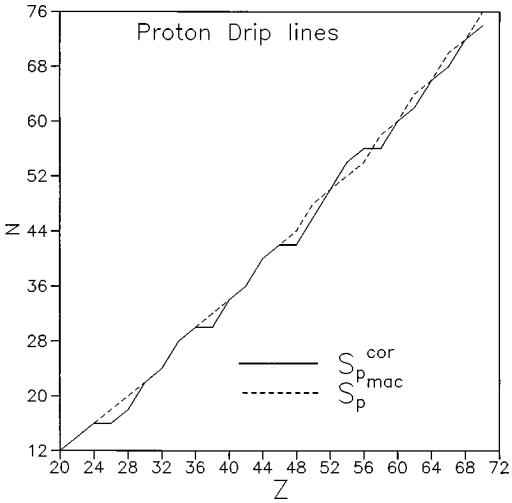

FIG. 2. Proton drip lines obtained by macroscopic separation energy and corrected separation energy.

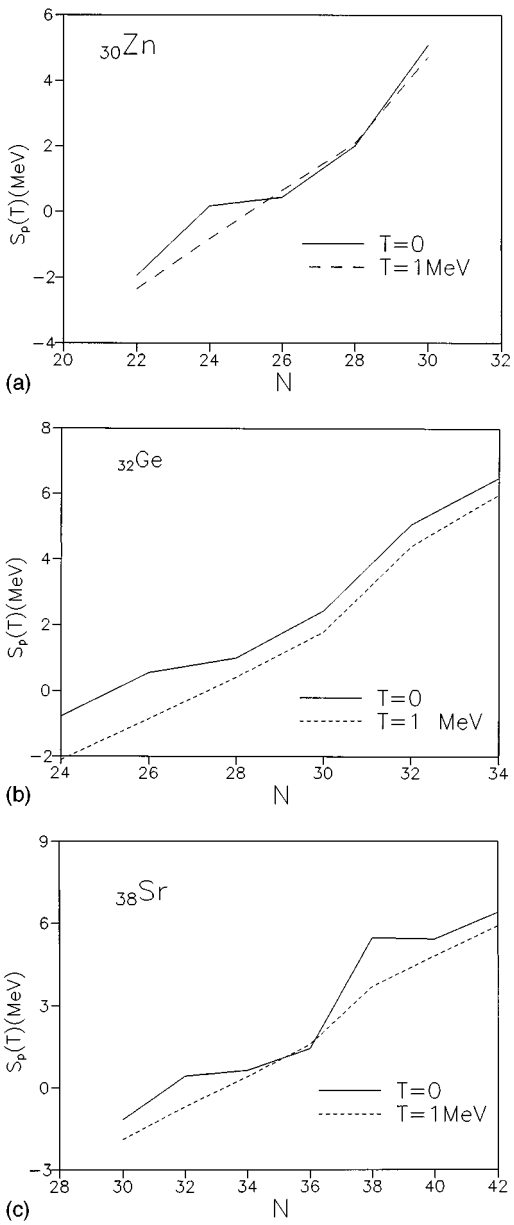

FIG. 3. (a) Plot of S_p vs neutron number for Zn at $T=0$ and 1 MeV. (b) Same as (a), but for Ge. (c) Same as (a), but for Sr.

In Fig. 2 we have traced the proton drip line from $Z=20$ to 70. Here we note that the inclusion of shell corrections alters the position of the drip line. The proton drip line obtained with the macroscopic mass formula is a smooth curve whereas the one obtained with $S_p^{\rm cor}$ fluctuates due to shell and deformation effects. Table I contains the values of corrected proton separation energy for nuclei from $Z=20$ to 40 lying on or close to the proton drip line along with the values of S_p from Ref. [7] which agree quite well with our results. Available experimental proton separation energies [31] are also given.

We found that astrophysically interesting [33] isotopes of ^{65}As and ^{69}Br with triaxial $(\theta=-160°,\ \delta=0.2)$ and oblate $(\theta=-180°,\ \delta=0.2)$ shapes, respectively, are unstable

TABLE I. Corrected proton separation energy for neutron deficient nuclei from $Z=20$ to 40 along with calculated values from Ref. [7] and available experimental [31] values of proton separation energy.

Z	A	S_p^{cor} (MeV)	S_p(calc.)[a] (MeV)	S_p(expt)[b] (MeV)	Z	A	S_p^{cor} (MeV)	S_p(calc.)[a] (MeV)	S_p(expt.)[b] (MeV)
20	32	−0.397			32	62	2.438	2.54	
20	34	2.045			32	64	5.053		5.0
20	36	4.108			32	66	6.490		6.2
20	38	5.404			33	61	−3.187	−2.7	
20	40	9.919			33	63	−1.860	−1.3	
22	36	−1.295			33	65	−0.595	−0.4	
22	38	0.671			33	67	2.190		
22	40	2.580			34	62	−0.239	−0.14	
22	42	4.071			34	64	0.997	1.0	
22	44	7.889			34	66	2.190	2.5	
24	40	−0.448			34	68	4.619		4.7
24	42	0.953			34	70	5.843		5.8
24	44	2.986			34	72	7.035		
24	46	4.818			35	65	−2.957	−2.8	
24	48	8.578			35	67	−1.583	−1.7	
26	42	−1.776			35	69	−0.502	−0.6	
26	44	0.021			35	71	3.571		
26	46	1.548	1.4		36	66	−0.528	−0.001	
26	48	2.993	2.7		36	68	1.171	1.3	
26	50	4.637			36	70	1.944		
26	52	7.592			36	72	4.993		4.67
28	46	−1.257			36	74	6.986		5.8
28	48	0.849	0.5		36	76	6.464		
28	50	1.920	1.5		38	68	−1.158		
28	52	2.985	2.6		38	70	0.428		
28	54	4.674			38	72	0.649		
28	56	8.170			38	74	1.428		
28	58	8.764			38	76	5.461		
30	52	−1.937	−2.1		38	78	5.425		5.9
30	54	0.171	−0.23		38	80	6.396		6.6
30	56	0.429	1.2		40	74	−0.177		
30	58	2.002			40	76	0.961		
30	60	5.085		5.1	40	78	2.075		
32	56	−0.775	−2.2		40	80	4.078		
32	58	0.546	−0.2		40	82	5.143		5.5
32	60	1.001	1.08		40	84	6.185		6.3

[a]See Ref. [7].
[b]See Ref. [31].

against proton emission with $S_p^{cor}<0$, in agreement with the prediction of Refs. [3,7,34,35]. However, the macroscopic separation energies of ^{65}As and ^{69}Br are found to be 324 keV and 418 keV, respectively, and hence are weakly bound under the macroscopic consideration.

III. STATISTICAL THEORY FOR HOT ROTATING NUCLEI

The grand partition function for a hot rotating nucleus is given by

$$Q(\alpha_Z,\alpha_N,\beta,\gamma)=\sum \exp(-\beta E_i+\alpha_Z Z_i+\alpha_N N_i+\gamma M_i). \tag{3.1}$$

where the Lagrangian multipliers α_Z, α_N, and γ conserve the number of protons, neutrons, and total angular momentum M of the system and are fixed by the following saddle-point equations:

$$-\partial \ln Q/\partial\beta=\langle E\rangle,$$

$$\partial \ln Q/\partial\alpha_Z=\langle Z\rangle,$$

$$\partial \ln Q/\partial\alpha_N=\langle N\rangle,$$

$$\partial \ln Q/\partial\gamma=\langle M\rangle. \tag{3.2}$$

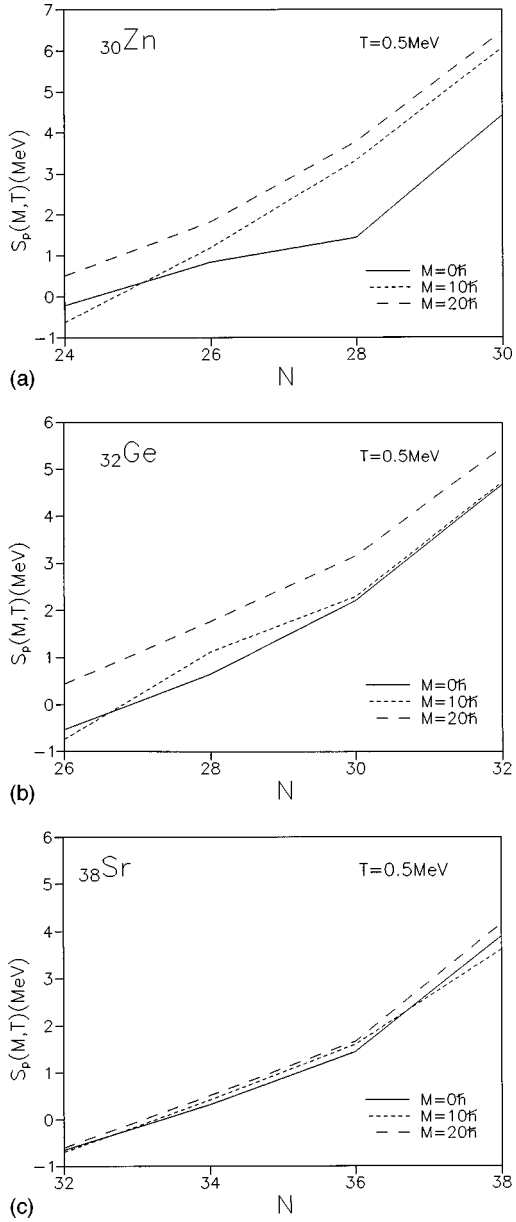

FIG. 4. (a) S_p vs N for different angular momenta $M=0$, $10\hbar$, and $20\hbar$ for Zn. (b) Same as (a), but for Ge. (c) Same as (a), but for Sr.

The corresponding equations in terms of single-particle levels for the protons ε_i^Z with spin projection m_i^Z, and neutrons ε_i^N with spin projection m_i^N [36], are

$$\langle Z\rangle=\sum\ n_i^Z=\sum\ [1+\exp(-\alpha_Z+\beta\varepsilon_i-\gamma m_i^Z)]^{-1}, \tag{3.3a}$$

$$\langle N\rangle=\sum\ n_i^N=\sum\ [1+\exp(-\alpha_N+\beta\varepsilon_i-\gamma m_i^N)]^{-1}, \tag{3.3b}$$

$$\langle E(M,T)\rangle=\sum\ n_i^Z\varepsilon_i^Z+\sum\ n_i^N\varepsilon_i^N, \tag{3.3c}$$

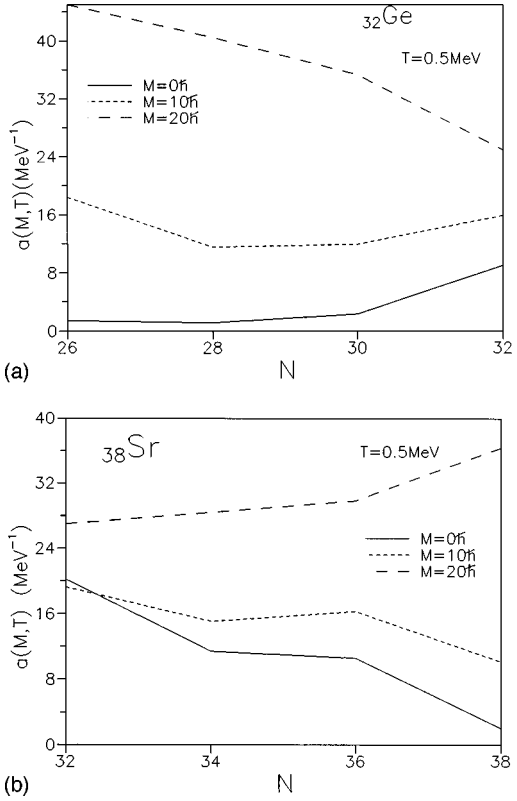

FIG. 5. (a) Level density parameter vs N for Ge at $T=0.5$ MeV and $M=0$, $10\hbar$, $20\hbar$. (b) Same as (a), but for Sr.

$$\langle M\rangle=\sum\ n_i^Z m_i^Z+\sum\ n_i^N m_i^N. \tag{3.3d}$$

The Lagrangian multiplier γ plays the same role as the rotational frequency ω in the cranking term ωJ of the cranked Nilsson Hamiltonian [37]; in fact, for biaxial deformation they are numerically equal as $T\rightarrow 0$.

When $M=0$, the thermal excitation energy $U(T)$ of the system is given by

$$U(T)=E(0,T)-E(0,0), \tag{3.4}$$

where $E(0,0)$ is the ground-state energy of the nucleus given as

$$E(0,0)=\sum_{i=1}^{Z}\ \varepsilon_i^Z+\sum_{i=1}^{N}\ \varepsilon_i^N. \tag{3.5}$$

The rotational energy $E_{\rm rot}$ is calculated using Eq. (3.3c)

$$E_{\rm rot}(M)=E(M,T)-E(0,T). \tag{3.6}$$

We define an effective excitation energy

$$U_{\rm eff}(T)=U(T)-\delta E_{\rm shell}, \tag{3.7}$$

where $\delta E_{\rm shell}$ is the ground-state shell correction. This is due to the fact that a part of the excitation energy is used to overcome the shell forces which are deformation dependent.

The total excitation energy is obtained using

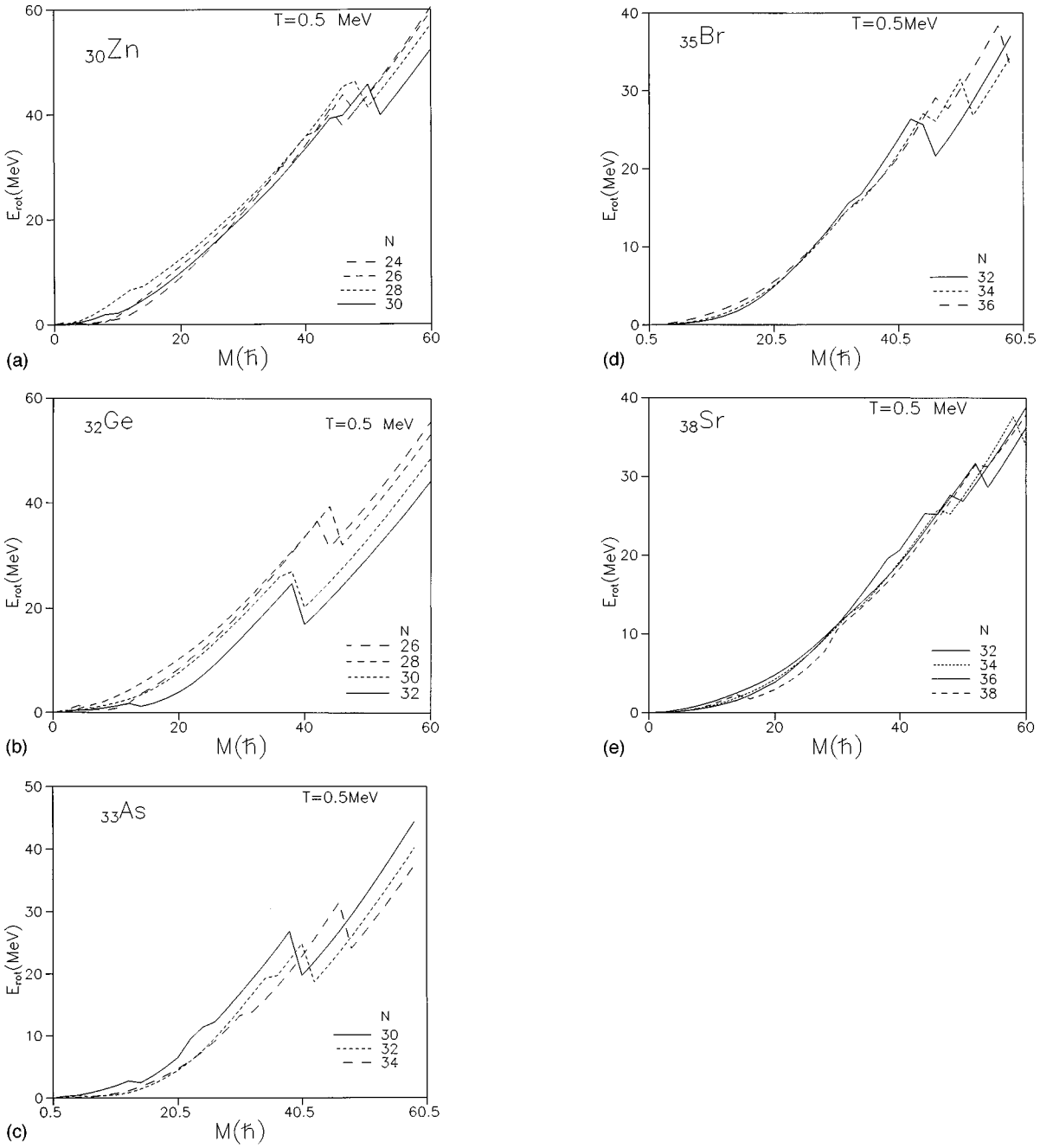

FIG. 6. (a) Rotational energy $E_{\rm rot}$ vs $M(\hbar)$ for Zn at $T=0.5$ MeV. (b) $E_{\rm rot}$ vs $M(\hbar)$ at $T=0.5$ MeV for Ge. (c) Same as (b), but for As. (d) Same as (b), but for Br. (e) Same as (b), but for Sr.

$$U(M,T)=U_{\rm eff}(T)+E_{\rm rot}(M). \tag{3.8}$$

The single-particle level density parameter $a(M,T)$ as a function of angular momentum M and temperature T is extracted using

$$a(M,T)=U(M,T)/T^2. \tag{3.9}$$

The nuclear level density $\rho(U)$ [36] for a nonrotating system $(M=0)$ is given as

$$\rho(U)=\frac{\sqrt{\pi}\,\exp(2\sqrt{aU})}{12U(aU)^{1/4}}, \tag{3.10}$$

whereas, in the case of a rotating system, $\rho(U)$ is evaluated using the expression [38]

$$\rho(U)=\frac{(\hbar^2/2\theta)^{3/2}(2I+1)\sqrt{a}\,\exp(2\sqrt{aU})}{12(U+T)^2}, \tag{3.11}$$

where the excitation energy $U=[E(M,T)-E(0,0)]-E_{\rm rot}$.

The moment of inertia θ is obtained with the expressions [39]

$$\theta_1=\hbar^2 I(dE_{\rm rot}/dI)^{-1}. \tag{3.12a}$$

$$\theta_2=\hbar^2(d^2E_{\rm rot}/dI^2)^{-1}. \tag{3.12b}$$

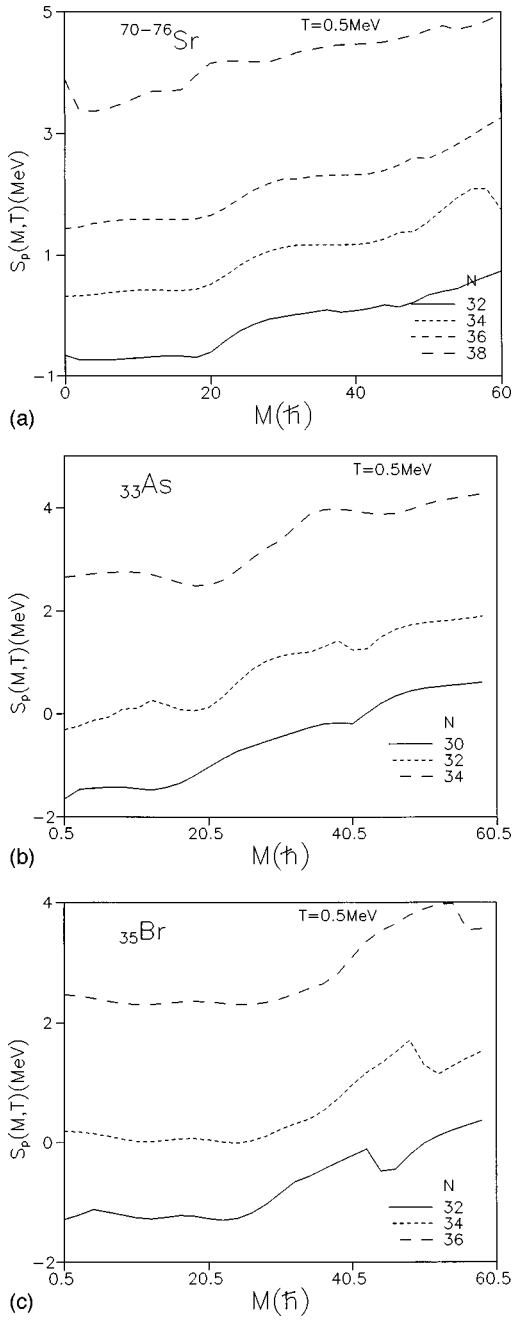

FIG. 7. (a) S_p vs $M(\hbar)$ for neutron deficient isotopes of Sr. (b) Same as (a), but for As. (c) Same as (a), but for Br.

Equation (3.12b) is used only when there is band crossing. Here $M=I+1/2$, as mentioned in Ref. [11].

The total binding energy of the system of N neutrons and Z protons at temperature T with angular momentum M, which should be maximized with respect to deformation parameter η, is given as

$$E_B(Z,N,T,M,\eta)=E_B(Z,N)-E_{\rm def}(\eta) - U(M,T,\eta)-E_{\rm rot}(M,\eta). \tag{3.13}$$

Here η refers to both angular and axial parameters.

The proton separation energy S_p, as a function of spin and temperature, is given by

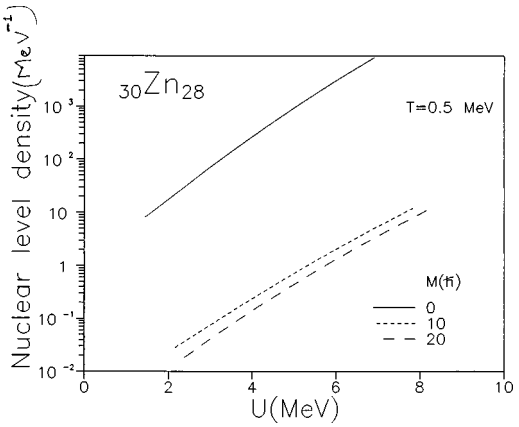

FIG. 8. Nuclear level density as a function of excitation energy U for $M=0$, $10\hbar$, and $20\hbar$ for $^{58}_{30}$Zn.

$$S_p(Z,N,T,M,\eta)=E_B(Z,N,T,M,\eta)-E_B(Z-1,N,T,M,\eta). \tag{3.14}$$

We present here the results on the effects of thermal and collective excitations on the proton separation energies and level density parameter of the neutron deficient nuclei Zn, Ge, As, Br, and Sr, lying on or close to the proton drip line.

Effects of temperature on the proton separation energy and proton drip line are shown in Figs. 3(a)–3(c) where the drip line is shifted towards the higher neutron number. For the even-even nuclei Zn, Ge, and Sr, the proton drip line is reached at $N=22$, 24, and 30, respectively, at $T=0$; at $T=1$ MeV, the drip line nuclei are with $N=24$, 26, and 32, respectively.

Proton separation energies of nuclei with $Z=30$, 32, and 38 for different spins $M=0$, $10\hbar$, and $20\hbar$ at $T=0.5$ MeV are shown in Figs. 4(a)–4(c). Here we observe that the proton separation energy increases significantly due to spin, especially near the magic neutron number $N=28$ for Zn. This may be due to the transition from spherical shape (at $M=0$) to oblate shape (at $M=10\hbar$). For $Z=38$, the change in S_p due to spin is not very significant up to $20\hbar$.

The level density parameter that carries with it the deformation-dependent shell effects affecting the separation energy is plotted in Figs. 5(a) and 5(b) for Ge and Sr.

Figures 6(a)–6(e) show the variation of $E_{\rm rot}$ with spin at $T=0.5$ MeV for neutron deficient nuclei Zn, Ge, As, Br, and Sr. We observe a dip in $E_{\rm rot}$ around $M=40-54\,\hbar$ due to a sudden rise in deformation suffered by the various isotopes of the above-mentioned nuclei. In $_{38}$Sr$_{34}$, at $M=60\hbar$, the equilibrium deformation rises suddenly to a value $\delta=0.6$, and $E_{\rm rot}$ drops and the separation energy S_p decreases by 0.3 MeV [see Fig. 7(a)].

In Sec. II, we observe that ^{65}As has ground-state (i.e., with $M,T=0$) separation energy $S_p^{\rm cor}<0$. As the spin increases to $8.5\hbar$, $S_p(Z,N,T,M,\eta)$ rises to a positive value and reaches a value 1.89 MeV at $58.5\hbar$. At $M=10.5\hbar$, it suffers a shape transition from triaxial ($\theta=-160°$) to oblate shape ($\delta=0.3$, $\theta=-180°$). At very high spins around $42.5\hbar$, the deformation parameter δ reaches an extremely large value. A similar change in deformation is observed in $^{67-71}$Br isotopes also around $52.5\hbar$–$58.5\hbar$. The nucleus ^{69}Br, which has negative ground state proton separation energy (at

$M=0$ and $T=0$) is weakly bound with $S_p(Z,N,T,M,\eta) = 0.188$ MeV at $T=0.5$ MeV and low spins $M \simeq 2\hbar$. As M increases further, $S_p(Z,N,T,M,\eta)$ increases and reaches a value 1.52 MeV at $58.5\hbar$. The equilibrium shape of ^{69}Br remains oblate ($\theta=-180°$) up to $M=58.5\hbar$. $S_p(Z,N,T,M,\eta)$ vs $M(\hbar)$ is plotted for neutron deficient isotopes of As and Br in Figs. 7(b) and 7(c). The proton separation energy S_p increases with neutron number and spin with small fluctuations.

Figure 8 shows the variation of nuclear level density as a function of excitation energy U for different spins. It is found that the nuclear level density increases with excitation energy for all spins. When $M=0$, all the excitation energy available to the system is entirely thermal and shows higher nuclear level density. As rotational energy increases, the nuclear level density is reduced due to part of the total energy being shared with the rotational degree of freedom.

IV. CONCLUSION

We have calculated one proton separation energy from the macroscopic-microscopic model for neutron deficient nuclei from $Z=20$ to 70. Shell structure and deformations of nuclei affect the proton separation energies and alter the drip line. Temperature and spin effects are incorporated. Proton separation energies are calculated for hot rotating neutron deficient nuclei Zn, Ge, As, Br, Sr. Thermal and rotational excitations alter the drip line.

ACKNOWLEDGMENTS

This work was supported by the University Grants Commission, India under the program of Special Assistance and the Committee on Strengthening the Infrastructure of Science and Technology (COSIST).

[1] C. Detraz *et al.*, Nucl. Phys. **A519**, 529 (1990).
[2] V. Borrel *et al.*, Z. Phys. A **344**, 135 (1992); R. J. Irvine *et al.*, Phys. Rev. C **55**, R1621 (1997).
[3] M. F. Mohar, D. Bazin, W. Benenson, D. J. Morrissey, N. A. Orr, B. M. Sherrill, D. Swan, J. A. Winger, A. C. Mueller, and D. Guillemaud-Mueller, Phys. Rev. Lett. **66**, 1571 (1991).
[4] J. A. Winger *et al.*, Phys. Lett. B **299**, 214 (1993).
[5] C. Detraz and D. J. Vieira, Annu. Rev. Nucl. Part. Sci. **39**, 407 (1989).
[6] E. Roeckl, Rep. Prog. Phys. **55**, 1661 (1992).
[7] W. E. Ormand, Phys. Rev. C **55**, 2407 (1991).
[8] R. Smolanczuk and J. Dobaczewski, Phys. Rev. C **48**, R2166 (1993).
[9] D. Hirata, H. Toki, T. Watabe, I. Tanihata, and B. V. Carlson, Phys. Rev. C **44**, 1467 (1991).
[10] P. Moller, J. R. Nix, W. D. Myers and W. J. Swiatecki, At. Data Nucl. Data Tables **59**, 185 (1995).
[11] M. Rajasekaran, T. R. Rajasekaran, N. Arunachalam, and V. Devanathan, Phys. Rev. Lett. **61**, 2077 (1988).
[12] M. Rajasekaran, T. R. Rajasekaran, P. Ratna Prasad, R. Premanand, D. Caleb Chanthi Raj and V. Devanathan, Nucl. Instrum. Methods Phys. Res. B **79**, 286 (1993).
[13] M. Faber and M. Ploszajazak, Z. Phys. A **291**, 331 (1979).
[14] M. Rajasekaran and Mamta Aggawal, Int. J. Mod. Phys. E **7**, 389 (1998).
[15] T. Ericson, Adv. Phys. **9**, 425 (1960).
[16] L. G. Moretto, Nucl. Phys. **A182**, 641 (1972).
[17] A. L. Goodman, Nucl. Phys. **A352**, 30 (1981).
[18] O. Civitarese and A. L. De Paoli, Nucl. Phys. **A440**, 480 (1985).
[19] O. Civitarese, A. Plastino, and A. Faessler, J. Phys. G **9**, 1063 (1983).
[20] M. Rajasekaran, T. R. Rajasekaran, and N. Arunachalam, Phys. Rev. C **37**, 307 (1988).
[21] M. Rajasekaran, N. Arunachalam, and V. Devanathan, Phys. Rev. C **36**, 1860 (1987).
[22] V. M. Strutinsky, Nucl. Phys. **A95**, 420 (1967).
[23] V. M. Strutinsky, Nucl. Phys. **A122**, 1 (1968).
[24] M. Brack, J. Damgaard, A. S. Jensen, H. C. Pauli, V. M. Strutinsky, and C. Y. Wong, Rev. Mod. Phys. **44**, 320 (1972).
[25] P. Moller and J. R. Nix, Nucl. Phys. **A361**, 117 (1981).
[26] F. Pougheon *et al.*, Nucl. Phys. **A327**, 17 (1987).
[27] P. A. Seegar, Nucl. Phys. **A238**, 491 (1975).
[28] G. Shanmugam, P. R. Subramanian, M. Rajasekaran, and V. Devanathan, *Nuclear Interactions*, Lecture Notes in Physics (Springer, Berlin, 1979), Vol. 72, p. 433.
[29] J. M. Eisenberg and W. Greiner, *Microscopic Theory of Nucleus* (North Holland, New York, 1976).
[30] D. L. Hill and J. A. Wheeler, Phys. Rev. **89**, 1102 (1953).
[31] A. H. Wapstra and G. Audi, Nucl. Phys. **A432**, 55 (1985).
[32] P. G. Henson and B. Jonson, Europhys. Lett. **4**, 409 (1987).
[33] R. K. Wallace and S. E. Woosely, Astrophys. J., Suppl. **45**, 389 (1981).
[34] J. D. Robertson *et al.*, Phys. Rev. C **42**, 1922 (1990).
[35] E. Hourani *et al.*, Z. Phys. A **344**, 277 (1989).
[36] J. B. Huizenga and L. G. Moretto, Annu. Rev. Nucl. Sci. **22**, 427 (1972).
[37] I. Hamamoto, in *Treatise on Heavy Ion Science*, edited by D. A. Bromley (Plenum, New York, 1984), Vol. 3.
[38] K. Snover, Annu. Rev. Nucl. Part. Sci. **36**, 545 (1986).
[39] I. Hamamoto, Phys. Scr. **T5**, 10 (1981).